Chemistry & Biology
Article

Sortin1-Hypersensitive Mutants Link Vacuolar-Trafficking Defects and Flavonoid Metabolism in *Arabidopsis* Vegetative Tissues

Abel Rosado,[1,6] Glenn R. Hicks,[1,6] Lorena Norambuena,[1,7] Ilana Rogachev,[2] Sagit Meir,[2] Lucille Pourcel,[3] Jan Zouhar,[4] Michelle Q. Brown,[1] Marietta P. Boirsdore,[1] Rachel S. Puckrin,[5] Sean R. Cutler,[1] Enrique Rojo,[4] Asaph Aharoni,[2] and Natasha V. Raikhel[1,*]

[1]Center for Plant Cell Biology and Department of Botany and Plant Sciences, University of California, Riverside, Riverside, CA 92521, USA
[2]Department of Plant Sciences, Weizman Institute of Science, Rehovot 76100, Israel
[3]Department of Plant Cellular and Molecular Biology and Plant Biotechnology Center, Ohio State University, Columbus, OH 43210, USA
[4]Departamento de Genética Molecular de Plantas, Centro Nacional de Biotecnología-CSIC, E-28049 Madrid, Spain
[5]Donnelly Centre for Cellular and Biomolecular Research, University of Toronto, Toronto, ON M5S 3E1, Canada
[6]These authors contributed equally to this work
[7]Present address: Laboratorio de Biología Molecular Vegetal, Departamento de Biología Facultad de Ciencias, Universidad de Chile, Las palmeras 3425 Ñuñoa, Santiago, Chile
*Correspondence: natasha.raikhel@ucr.edu
DOI 10.1016/j.chembiol.2010.11.015

SUMMARY

Sortin1 is a chemical genetic-hit molecule that causes specific mislocalization of plant and yeast-soluble and membrane vacuolar markers. To better understand its mode of action, we designed a Sortin1-hypersensitive screen and identified several Sortin1-hypersensitive and flavonoid-defective mutants. Mechanistically, Sortin1 mimics the effect of the glutathione inhibitor buthionine sulfoximine and alters the vacuolar accumulation of flavonoids, likely blocking their transport through vacuole-localized ABC transporters. Structure-activity relationship studies conducted in *Arabidopsis* revealed the structural requirements for Sortin1 bioactivity and demonstrated that overlapping Sortin1 substructures can be used to discriminate between vacuolar-flavonoid accumulations and vacuolar-biogenesis defects. We conclude that Sortin1 is a valuable probe for dissecting novel links among flavonoid transport, vacuolar integrity, and the trafficking of vacuolar targeted cargoes in *Arabidopsis*.

INTRODUCTION

Endomembrane trafficking in eukaryotes is fundamental for the intracellular delivery of soluble and membrane cargoes, secretion, and endocytosis (Surpin and Raikhel, 2004). The importance of the secretory apparatus in plants is highlighted by the fact that proper vacuole biogenesis is essential in plants (Rojo et al., 2001) yet dispensable in yeast (Horazdovsky and Emr, 1993). In fact, loss-of-function mutations affecting the plant secretory system components frequently result in reduced embryo viability (Rojo et al., 2001) and male gametophyte function (Sanderfoot et al., 2001), as well as other defects leading to lethality (Hicks et al., 2004). While demonstrating the essentiality of the secretory pathway, these findings point to a limitation of classical genetic approaches for understanding plant secretion because lethal or poorly heritable mutations are particularly challenging to study. Another limitation of classical genetic approaches in plants is that loss-of-function mutations frequently fail to result in detectable phenotypes due to extensive gene or functional redundancy (Surpin et al., 2003). To advance beyond such limitations, biologists and chemists are rediscovering the value of small molecules in understanding basic biological processes, and libraries of small molecules have been recently used to probe the biology of the secretory system in *Arabidopsis* (Park et al., 2009; Hicks and Raikhel, 2010).

In a previous study we took advantage of the conservation of endomembrane components between yeast and plants to screen for chemicals affecting the targeting of soluble vacuolar proteins in the yeast *Saccharomyces cerevisiae* and *Arabidopsis*. This effort identified three compounds (Sortin1, Sortin2, and Sortin3) that resulted in pronounced defects in vacuole biogenesis and inhibition of root growth in *Arabidopsis* seedlings (Zouhar et al., 2004). The versatility of Sortins for dissecting pathways in different biological contexts was demonstrated by the use of Sortin2 to identify elements of the endomembrane system in yeast (Norambuena et al., 2008), and the use of Sortin3 to dissect the compartmentalization and export of secondary metabolites in the filamentous fungus *Aspergillus parasiticus* (Chanda et al., 2009). In this study we designed a Sortin1-hypersensitive screen to identify pathways important for the delivery of vacuolar cargoes in *Arabidopsis*. Our screen used an EMS-mutagenized population expressing the δ-tonoplast intrinsic protein fused with the green fluorescent protein (δ-TIP: GFP), which enabled rapid visualization of vacuolar morphology in candidate mutants (Cutler et al., 2000). This screen revealed that Sortin1-hypersensitive mutants with severe vacuolar-morphology phenotypes also possess flavonoid accumulation defects, suggesting a prominent role of the flavonoid biosynthesis/transport machinery for vacuolar biogenesis and vacuolar cargo delivery in *Arabidopsis* vegetative tissues.

In addition to acting as pigments in fruits and flowers, flavonoids are involved in a vast array of other biological functions such as symbiotic plant-microbe interactions (Steinkellner et al., 2007), auxin transport (Peer and Murphy, 2007), defense (Treutter, 2005), and protection against oxidative damage (Taylor and Grotewold, 2005). The wide variety of flavonoids derives from the phenylpropanoid pathway, which is one of the most thoroughly studied enzymatic pathways in plants. In this pathway, flavonoids appear to be synthesized by the action of a multienzyme complex associated with the cytoplasmic face of the endoplasmic reticulum (ER) (Winkel, 2004) and are transported from the ER to the large central vacuole. Although the biosynthetic elements of the flavonoid pathway have been thoroughly described (Winkel-Shirley, 2001; Pourcel et al., 2007; Martens et al., 2010), their mechanisms of transport and vacuolar accumulation remain unclear, and two nonexclusive models have been proposed (Zhao et al., 2010). The first model suggests the existence of a vesicular-type transport of flavonoids from the ER to the vacuole that utilizes components of protein secretory trafficking and does not require the presence of carrier proteins or tonoplast transporters (Poustka et al., 2007). The second model suggests that the vacuolar transport of flavonoids occurs through either directly energized ABC-type transporters (Yazaki, 2006) or secondarily energized multidrug and toxic compound extrusion (MATE) antiporters, which are usually driven by the H^+ gradient across the tonoplast (Baxter et al., 2005; Marinova et al., 2007). For both models, available data suggest that the conjugation of moieties such as sugars, acyl residues, or glutathione is an important determinant for increasing the flavonoids solubility, reducing toxicity, and determining vacuolar transport (Zhao and Dixon, 2010).

In this study the identification of multiple Sortin1-hypersensitive and flavonoid-defective mutants, together with the Sortin1 structure-activity relationship (SAR) analysis, allowed us to characterize a crosstalk between flavonoid transport and the delivery of vacuolar cargoes in vegetative tissues. In agreement with previous models of detoxification of xenobiotics, we hypothesize that the oxidative damage caused by Sortin1 depletes the cytosolic glutathione pools, blocks the vacuolar accumulation of flavonoids through ABC-type tonoplast transporters, affects vacuolar biogenesis, and influences the fate of vacuolar-targeted cargoes. Moreover, SAR analyses identified a 1, 4-dihydroindeno [1, 2-b] pyridin-5-one substructure (from now on, Substructure A) as an essential requirement for Sortin1 bioactivity.

RESULTS

Sortin1 Alters Vacuolar Morphology and the Delivery of Vacuolar Cargoes

Sortin1 was initially identified as a compound that alters the N-terminal propeptide-mediated transport (NTPP transport) of the carboxypeptidase Y cargo to yeast and *Arabidopsis* vacuoles (Zouhar et al., 2004). To test whether this effect was specific for the NTPP vacuolar-trafficking pathway, we investigated the effect of Sortin1 on delivery of a marker protein using the C-terminal propeptide pathway (CTPP), a plant-specific vacuolar-targeting pathway. For this purpose we performed immunoelectron microscopy of a genetically engineered small protein, CLV3, fused with the T7 tag and the barley lectin C-terminal vacuolar-sorting signal (CLV3: T7:$CTPP_{BL}$), a marker used for the identification of components involved in the vacuolar sorting of CTPP-containing proteins (Sohn et al., 2007; Rosado et al., 2010). As shown in Figures S1A–S1C (available online), Sortin1 treatments caused a significant redirection of the T7-immunogold labeling to the root apoplast, indicating that both CTPP and NTPP vacuolar-trafficking pathways are affected by Sortin1 treatments in *Arabidopsis*.

Once we determined that Sortin1 alters the vacuolar delivery of NTPP and CTPP-containing proteins, we examined its impact on the morphology of the vacuole and other endomembrane compartments using various endomembrane markers. These experiments show that the localization patterns of GFP: KDEL (an ER lumen marker) (Fluckiger et al., 2003) (Figures 1A and 1B) and GFP: NAG1 (a Golgi marker) (Grebe et al., 2003) (Figures 1C and 1D) were unaffected by 57 μM (25 μg/ml) Sortin1 treatments (Figures 1A–1D), a concentration sufficient to cause both root elongation and vacuolar-morphology defects (Zouhar et al., 2004). No effects of Sortin1 were observed on the localization of the *trans*-Golgi network (TGN) and prevacuolar compartment (PVC) marker *SYP61* (CFP: SYP61; Robert et al. [2008]) (Figures 1E and 1F), or the plasma membrane marker PIP2a (GFP: PIP2a) (Cutler et al., 2000) (Figures 1G and 1H). However, Sortin1 treatments resulted in significant disruption of vacuole morphology, as indicated by two tonoplast-specific markers (GFP: γ-TIP and GFP: δ-TIP) (Cutler et al., 2000) (Figures 1I–1L). Collectively, our microscopy-based observations show that Sortin1 specifically disrupts vacuolar morphology without affecting other secretory compartments.

Screen for Sortin1-Hypersensitive Mutants

Sortin1 perturbs the CTPP and NTPP-trafficking pathways, and its application causes specific aberrant localization of tonoplast markers. Therefore, we reasoned that weak mutants in essential vacuolar-trafficking factors would be enhanced by the addition of Sortin1. To identify those elements we generated an EMS-mutagenized GFP: δ- TIP *Arabidopsis* collection and used sublethal doses of Sortin1 in a hypersensitive screen. First, we performed a dose-response experiment using the parental GFP: δ- TIP line and determined that root-elongation inhibition could be a visible marker that allows the rapid identification of hypersensitive mutants in the primary screen (Figures S1D–S1K). Next, we determined that 11 μM Sortin1 (a concentration that resulted in little or no vacuolar-biogenesis defects and no inhibition of root growth in wild-type plants) was a suitable concentration for the hypersensitive screen (Figures S1F and S1G).

After a primary screen of 112,000 EMS-mutagenized GFP:δ-TIP seedlings, 360 putative mutants were selected, and their progenies were rescored for root-elongation inhibition (Figures S1L–S1O). After the secondary screen, 121 lines were retained as putative Sortin1-hypersensitive mutants (*s1h)*. Next, normalized ratios were calculated as the mean root length in the presence of 11 μM Sortin1 divided by the mean root length in control media, and a cutoff ratio of 2 was arbitrarily selected to define six strong Sortin1-hypersensitive mutants (Figure 1M), which were examined for GFP: δ-TIP localization in the presence of Sortin1. This revealed that they all presented vacuolar-biogenesis defects in hypocotyls at 11 μM Sortin1, in contrast to the higher

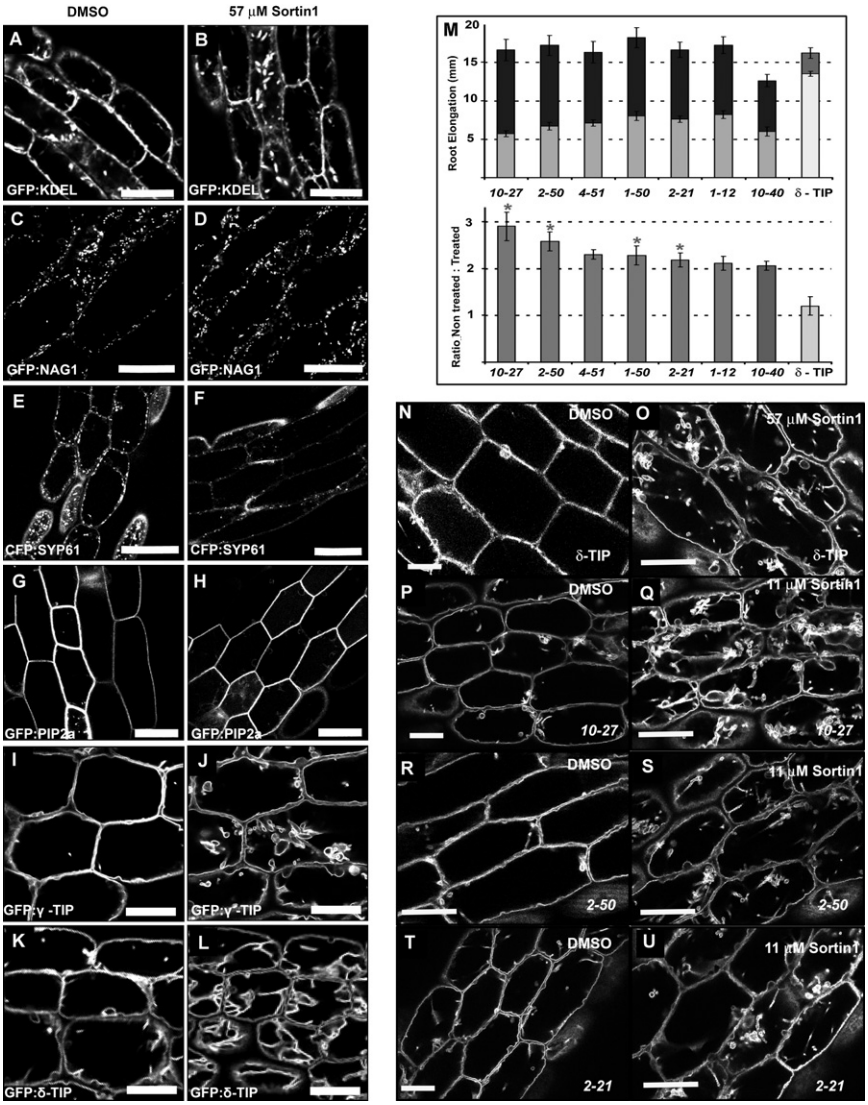

Figure 1. Sortin1-Hypersensitive Screen

(A–L) Sortin1 affects vacuole morphology specifically. Seedlings expressing different endomembrane-protein fusions were grown in the absence or presence of 57 μM (25 μg/ml) Sortin1, and hypocotyls were imaged after 6 days. The markers used were: GFP: KDEL (ER) (A and B); GFP: NAG1 (Golgi) (C and D); CFP: SYP61 (Golgi, PVC, TGN) (E and F); GFP: PIP2a (PM) (G and H); GFP: γ-TIP-like (tonoplast) (I and J); or GFP: δ-TIP (tonoplast) (K and L).

(M) Root elongation is used as a marker in the Sortin1-hypersensitive screen. In the top panel, mean root lengths of the seven most hypersensitive mutants (M3 generation) were estimated in the absence (dark gray) or presence (light gray) of 11μM (5 μg/ml) Sortin1 (n = 15–20). The mean length of the GFP: δ-TIP control line is indicated in lighter tones.

Error bars represent the standard deviation of the data (n = 15–20). In the bottom panel a ratio was calculated as the mean root length in the presence of 11 μM Sortin1 divided by the mean root length in DMSO. Error bars represent the standard deviation of the ratios (n = 3). Hypersensitive mutants with ratios over two were selected as hypersensitive to Sortin1. Asterisks indicate mutants with aberrant seed color. The *s1h2-50* and *s1h1-50* mutants were siblings, and only *s1h2-50* was selected for further characterization.

(N–U) Tonoplast morphology of the Sortin1-hypersensitive mutants was examined by confocal microscopy. GFP: δ-TIP (N and O) grown for 6 days in the absence or presence of 57μM (25μg/ml) Sortin1, and the Sortin1-hypersensitive mutants *s1h10-27* (P and Q), *s1h2-50* (R and S), and *s1h2-21* (T and U) in the absence or presence of 11μM (5μg/ml) Sortin1. Scale bars, 40 μm. (See also Figure S1.)

Sortin1 (57 μM) required for the wild-type GFP: δ-TIP parental line (compare wild-type Figures 1N and 1O with examples in Figures 1P–1U). These results confirm that the root-elongation inhibition and vacuolar-biogenesis defects are associated phenotypes caused by the Sortin1 treatments.

Several *s1h* Mutants Have Defects in Flavonoid Biosynthesis and Their Vacuolar Transport

A phenotype that differentiated the *s1h* mutants and allowed their separation into different complementation groups was the seed color. As observed in Figure 2A, the color of the selected *s1h* mutants varied from the wild-type brown (*s1h4-51*, *s1h1-12*, and *s1h10-40*) to pale yellow (*s1h2-50*), with intermediate pigmentations such as grayish-green (*s1h2-21*) or light brown (*s1h10-27*). To test whether the *s1h2-50*, *s1h2-21*, and *s1h10-27* mutations were allelic, genetic analyses using the six possible cross combinations were performed. As shown in Table S1, all F1 seed coats from the crosses showed maternal characteristics, the F2 segregant populations displayed normal seed coats, and the F3 populations showed differentiated progenies with maternal or paternal features. These results combined with the genetic analysis of the vacuolar-biogenesis defects (Table S2) indicated that the *s1h10-27*, *s1h2-50*, and *s1h2-21* mutations were recessive and nonallelic.

Because multiple mutants with aberrant seed colors have been related with deficient flavonoid biosynthesis and transport (Lepiniec et al., 2006), we tested whether the *s1h* mutants were affected in the flavonoid pathway. For this purpose we used the aromatic aldehyde *p*-dimethylaminocinnamaldehyde (DMACA) that specifically reacts with proanthocyanidins, flavan-3,4-diols, and flavan-3-ols, giving a positive reaction indicated by the dark-purple/brown color in mature seeds (Abrahams et al., 2003). When mature *s1h* seeds were stained with DMACA, a positive reaction similar to that of wild-type was detected for *s1h4-51*, *s1h1-12*, and *s1h10-4*. In contrast, *s1h2-50* seeds were negative for the DMACA staining, and the *s1h10-27* and *s1h2-21* seeds displayed dark patches in the radicle protrusion area, suggesting that flavonoid synthesis was still occurring but to a lesser extent

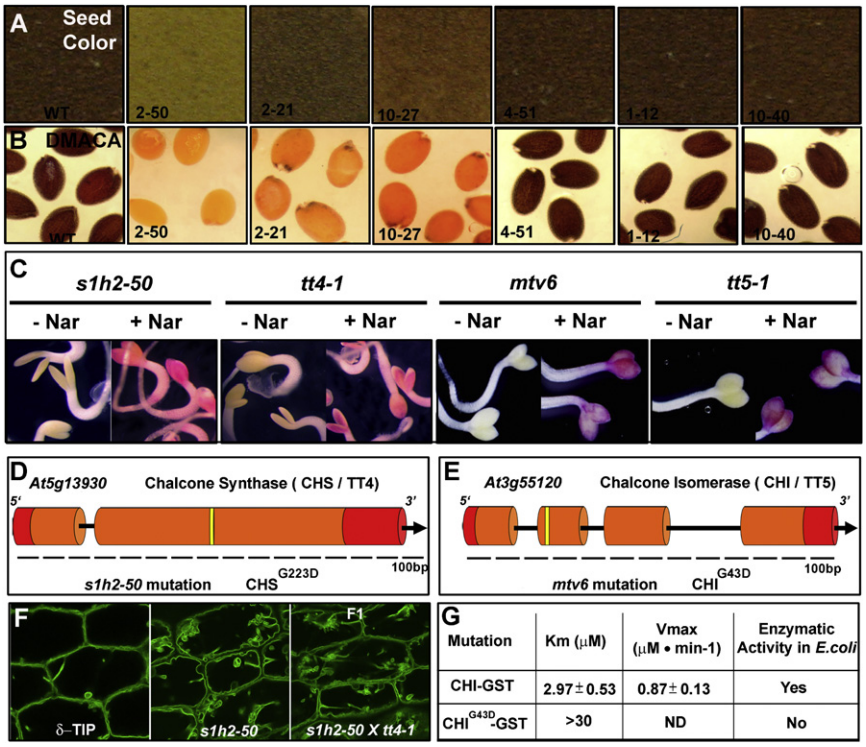

Mutation	Km (μM)	Vmax (μM • min-1)	Enzymatic Activity in *E.coli*
CHI-GST	2.97±0.53	0.87±0.13	Yes
CHI^{G43D}-GST	>30	ND	No

Figure 2. A Subgroup of Sortin1-Hypersensitive Mutants Is Affected in Flavonoid Biosynthesis and Transport

(A) Seed color.

(B) DMACA staining. The dark coloration of the seeds indicates vacuolar accumulations of proanthocyanidins.

(C) Chemical complementation of *s1h2-50*, *tt4-1*, mtv6, and *tt5-1* mutants with naringenin. Phenotype of 6-day-old seedlings grown under AICs in the absence (−Nar) or presence (+Nar) of naringenin. The pink color indicates vacuolar accumulations of pigmented anthocyanins.

(D and E) Targeted sequencing identifies *s1h2-50* and *mtv6* as *tt4* and *tt5* mutant alleles, respectively. The figures represent the exon-intron organization and schematic representation of the locations of the mutations in *s1h2-50* and *mtv6*. Orange, exon; black, intron; red, untranslated region; yellow, mutation positions.

(F) Allelism test. The tonoplast morphology defects are associated with mutations in *tt4*. The recessive mutants *s1h2-50* (carrying the δ-TIP:GFP marker) and *tt4-1* were crossed, and the F1 population was analyzed for mislocalization of the δ-TIP:GFP tonoplast marker.

(G) Chalcone isomerase enzymatic assay. In vitro enzyme kinetic analyses were carried out on *E. coli*-expressing GST-tagged recombinant proteins CHS and CHS^{G43D} (*mtv6*). The substrate concentration in the reaction mixture was monitored at the isosbestic point at 333 nm, and velocity was expressed as micromoles of chalcone consumed/min.

See also Figure S2 and Tables S1–S3.

than in the wild-type (Figure 2B). Therefore, we concluded that *s1h2-50*, *s1h10-27*, and *s1h2-21* were elements of the general flavonoid biosynthesis/transport pathways. Interestingly, another flavonoid-defective mutant, modified transport to the vacuole 6 (*mtv6*), was isolated in an independent screen for mutants that cause aberrant secretion of the vacuolar-targeted CLV3: T7: CTPP$_{BL}$ cargo in vegetative tissues (Sohn et al., 2007; Rosado et al., 2010) (Figures S2A–S2D), strengthening the conclusion that flavonoid metabolism is important for vacuolar trafficking.

Identification of the *s1h2-50* and *mtv6* Mutants

Under anthocyanin-inductive conditions (AICs) (Poustka et al., 2007), wild-type seedlings displayed pink coloration due to the vacuolar accumulation of pigmented anthocyanins (Figure S2E); however, *s1h2-50* and *mtv6* seedlings grown in similar conditions failed to accumulate pigments (Figure 2C). This phenotype was reversed by the addition of the flavonoid precursor naringenin, as previously described in mutants localized upstream of this intermediate in the flavonoid biosynthetic pathway such as the chalcone synthase *CHS tt4-1* (CS8605) and the Chalcone Isomerase *CHI tt5-1 (CS86)* enzymes (Shirley et al., 1995, Poustka et al., 2007) (Figure 2C; Figures S2F and S2G). Indeed, sequencing of the genes encoding these enzymes in the *s1h2-50* and *mtv6* mutant backgrounds revealed that *s1h2-50* is a mutant allele of the CHS/TT4 enzyme harboring a mutation in close proximity to the gatekeeper CHS^{F220} residue (Dana et al., 2006) (CHS^{G223D}, Figure 2D), and also identified *mtv6* as a mutant allele of the CHI/TT5 enzyme (CHI^{G43D}) (Figure 2E) harboring a mutation in the β3 sheet, a component of the CHI active site on the protein surface (Jez et al., 2000). Allelism tests between *s1h2-50* and *tt4-1* confirmed that the vacuolar-biogenesis defects were due to mutations in the *CHS* gene (Figure 2F), and biochemical analyses demonstrated that the CHI^{G43D} mutation in *mtv6* caused the loss of enzymatic activity and inhibited the conversion of the CHI substrate to naringenin in *E. coli* (Figure 2G). These results strongly support a direct role for flavonoids in vacuolar biogenesis and the delivery of vacuolar cargoes in *Arabidopsis* (summary of mutant phenotypes can be found in Table S3).

Sortin1 Inhibits the Vacuolar Accumulation of Flavonoids

The Sortin1-hypersensitive screen resulted in three independent mutants with flavonoid biosynthesis or accumulation defects, so we questioned whether Sortin1 alters the vacuolar accumulation of flavonoids by either inhibiting their biosynthesis or transport in vegetative tissues. To answer this question we analyzed the concentrations of pigmented anthocyanins in Sortin1-treated seedlings grown under AICs (Figures 3A–3D). Compared with untreated seedlings (Figure 3A), AIC-grown seedlings supplemented with 57 μM Sortin1 significantly reduced the vacuolar accumulation of pigmented anthocyanins (estimated as the amount of anthocyanidins produced by acid hydrolysis) (Rabino

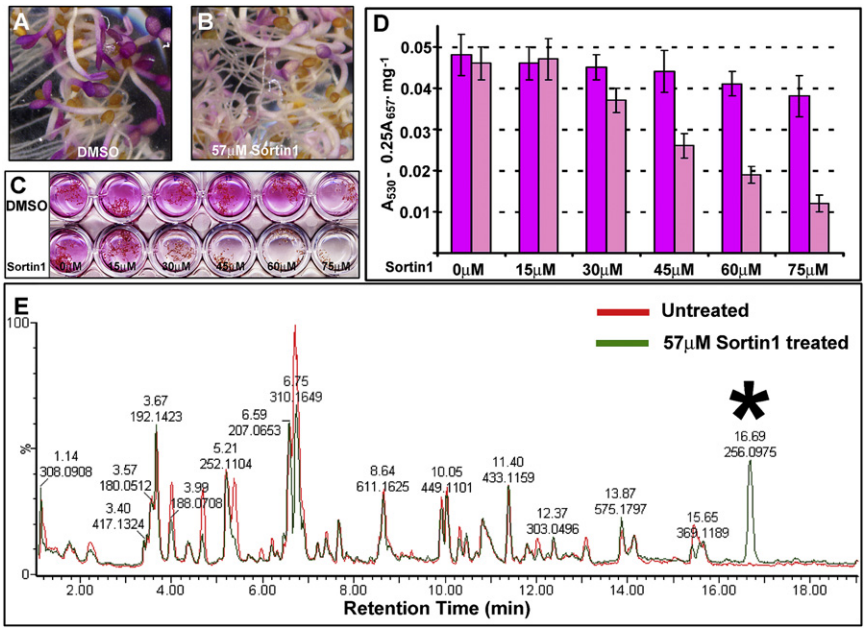

Figure 3. Sortin1 Inhibits the Vacuolar Accumulations of Pigmented Anthocyanins

(A and B) Vacuolar accumulation of pigmented anthocyanins in AIC-grown seedlings in the absence (A) or presence (B) of 57 μM Sortin1.

(C) Colorimetric assay for anthocyanin accumulation in the presence of DMSO (upper row) or different concentrations of Sortin1 (lower row).

(D) Spectrophotometric measurement of anthocyanin accumulations of AIC-grown wild-type (δ-TIP) seedlings incubated in the absence (dark-pink bars) or presence (light-pink bars) at different Sortin1 concentrations. For every concentration, error bars represent the standard deviation of three independent experiments (n = 3).

(E) LC-MS profiling of flavonols and anthocyanins from AIC-grown wild-type (δ-TIP) seedlings treated with DMSO (red) or Sortin1 (green) for 24 hr. The numbers in the chromatogram correspond to retention times (upper) and masses (lower). The asterisk (*) indicates a Sortin1 light-accelerated hydrolysis product (m/z 256).

See also Tables S4 and S5 for the list of anthocyanins and flavonols putatively identified by MS-MS analysis.

and Mancinelli, 1986) (Figure 3B). This reduction was dose dependent as estimated both qualitatively, using a colorimetric assay (Figure 3C), and quantitatively, using normalized spectrophotometric measurements (Figure 3D). Next, we determined whether flavonoid biosynthesis was also affected by Sortin1 treatments. For that purpose the flavonoid profiles of Sortin1-treated and untreated seedlings were compared using ultra-performance liquid chromatography coupled to time-of-flight mass spectrometry (UPLC-QTOF-MS analysis). As shown in Figure 3E, the flavonoid profiles of Sortin1-treated and untreated seedlings were nearly identical with the exception of clear peak that appeared in the Sortin1-treated plants (asterisk, discussed later). Peak identification by MS fingerprinting followed by semiquantitative analysis of the MS data suggested no accumulation of flavonoid intermediates and only a mild reduction on quercetin derivatives (10%–20% reductions) (Tables S4 and S5) after Sortin1 treatment. Taken together, these results suggest that Sortin1 has a limited effect on flavonoid biosynthesis and an inhibitory role on flavonoid-derivative transport.

Sortin1 Mimics the Effects of the Glutathione-Biosynthesis Inhibitor Buthionine Sulfoximine

Sortin1 inhibits the vacuolar accumulation of flavonoids, a process proposed to occur through ABC-type tonoplast transporters in vegetative tissues (Yazaki, 2006), so we investigated whether Sortin1 interferes with the activity of ABC transporters. To do so, we compared the physiological effects of Sortin1 with those of the known ABC transporter inhibitor BSO.

In terms of development the similarities of the Sortin1 and BSO treatments were evident because both treatments caused reduction of the primary root growth (Koprivova et al., 2010) (Figures S1D–S1K), and inhibition of the root-hair elongation (Figures 4A–4C). In terms of flavonoid accumulations, both treatments caused a mosaic of cells with punctate accumulations of pigmented anthocyanins in cotyledons (Figures 4D–4F). Interestingly, similar anthocyanin accumulations were also observed when using the more general ABC transporter inhibitor vanadate (Na_3VO_4); however, the bathochromic shift (from purple red to bluish) that reflects the alkalinization of the vacuole in Na_3VO_4-treated seedlings was not observed, neither on Sortin1 nor on BSO treatments (Poustka et al., 2007) (Figure S3A). Microscopically, Sortin1 and BSO treatments were also similar, and both induced the formation of neutral red-staining bodies (NRSBs) (Poustka et al., 2007) (Figures 4G–4I) that were characterized as dynamic structures with elevated concentrations of anthocyanins (Figures 4J–4L; Figure S3B). Similar structures have been previously described as a result of physiological responses to light and oxidative stress, and also appear in mutants with enhanced autophagy (Irani and Grotewold, 2005, Poustka et al., 2007, Pourcel et al., 2010). Another phenotype that could be associated with oxidative stress and autophagy responses was the enhanced tonoplast vesiculation observed in Sortin1 and BSO-treated seedlings grown in AICs (Figures 4M–4O). Finally, at the regulatory level, microarray analyses indicate that Sortin1 treatments induced the expression of P450-dependent monoxygenases, glutathione S-transferases, and glucosyltransferases. Similar gene classes were induced by BSO (Koprivova et al., 2010) (Table S6), as well as by the xenobiotic Trinitrotoluene (TNT), a known generator of oxidative stress in plants (Gandia-Herrero et al., 2008) (Table S6). Based on these results, we postulate that Sortin1 is an oxidative stress generator that could inhibit the vacuolar transport of flavonoids by depleting the GSH pools or inhibiting GST function in a similar manner as BSO.

SARs Identify Elements Required for Sortin1 Bioactivity

Sortin1 is unstable in *Arabidopsis* growth media, its decomposition is likely favored by the rearomatization of the pyridine ring in the 1, 4-dihydroindeno [1, 2-b] pyridin-5-one backbone (putative substructure A, Figure 5A), and its reactivity is enhanced in the

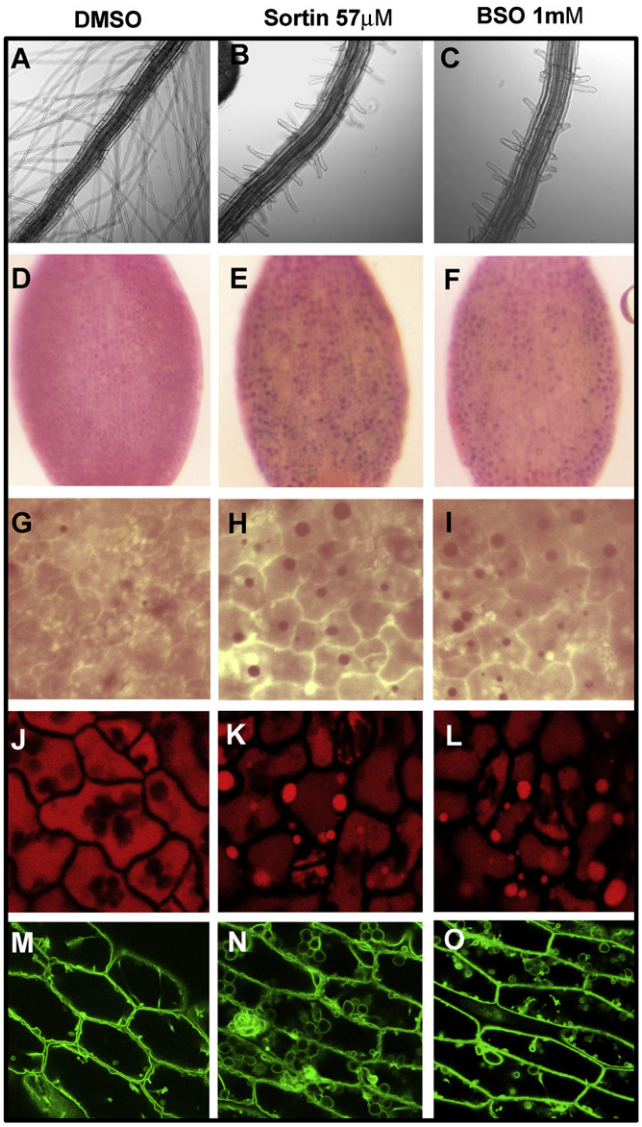

Figure 4. Sortin1 Phenotypes Resemble those of the Glutathione Inhibitor BSO

(A–C) Root-hair elongation defects in seedlings.

(D–F) Heterogeneous distribution of pigmented anthocyanins.

(G–I) Formation of NRSBs in cotyledons. Seedlings were treated for 24 hr with DMSO, Sortin1, or BSO and stained for 20 min with neutral red (1 mg/ml).

(J–L) Accumulation of fluorescence in NRSBs. Naringenin-treated AIC-grown wild-type seedlings were incubated for 24 hr in the presence of DMSO, Sortin1, or BSO. Anthocyanins were excited with a 543 nm line from a He-Ne laser, and fluorescence was detected in the 565–620 nm range.

(M–O) Tonoplast vesiculation. Six-day-old AIC-grown *Arabidopsis* seedlings expressing the GFP: δ-TIP markers were incubated for 24 hr in the presence of DMSO, Sortin1, or BSO, and fluorescence was analyzed using confocal microscopy.

See also Figure S3 and Table S6.

presence of water and light (Figures 5A and 5B; Figure S4A–S4F). Indeed, the Sortin1 standard peak detected in DMSO solutions (RT = 35.48 min, m/z 440.11) disappears after hydrolysis, and the putative Substructure A (RT = 27.33 min, m/z 254.08) appears to be the most abundant Sortin1 derivative in these conditions (Figure 5A; Figure S4B). Because Sortin1 derivatives can be detected in vivo (Figure 3A), we hypothesized that the putative Substructure A, corresponding to the most abundant Sortin1 hydrolysis product, could be the bioactive molecule causing the observed phenotypes. To test this hypothesis we performed SAR analyses and identified eight additional chemicals (designated with ChemBridge numbers) similar in structure or representing Sortin1 substructures (Table 1). Next, we determined their bioactivity considering as bioactive those chemicals showing equal or higher chemical potency than Sortin1 in terms of δ-TIP: GFP mislocalization and/or inhibition of the vacuolar accumulation of pigmented anthocyanins (Figures 5C and 5D and Table 1; Figure S4G). As shown in Table 1 and Figure 5C, only 6177037 (**6,** Table 1), that differentiated from Sortin1 in the position of the carboxyl group, and 6980879 (**2,** Table 1), that represented most of Sortin1 minus the benzoic acid group on the furan ring, were considered bioactive in terms of vacuolar biogenesis. Similarly to Sortin1, structures **2** and **6** were unstable in aqueous solution (Figure 5B) and potentially generated Substructure A- like compounds required to cause vacuolar-biogenesis defects (Figure 5E, top). In terms of accumulation of pigmented anthocyanins, the analogs and substructures **2, 4**, and **6–9** were bioactive to a similar extent than Sortin1 (Table 1 and Figures 5D; Figure S4G). The comparative analysis of those substructures suggested that the nonsubstituted Substructure 4 (Table 1) was sufficient to cause anthocyanin-accumulation defects (Figure 5E, bottom). Still, the identity of the bioactive substructures has to be further confirmed using more accurate techniques such as nuclear magnetic resonance (NMR).

DISCUSSION

Sortin1 Defines a Crosstalk between Vacuolar Transport and Flavonoid Accumulation

Chemical genomic approaches have recently emerged as powerful tools to dissect processes that may be intractable using conventional genetics because of gene lethality or redundancy. To understand and dissect complex biological processes and crosstalk between pathways, several screens for bioactive chemicals have been recently reported, and compounds that affect auxin responses, cytoskeleton, cell wall, and plant growth have been identified (reviewed in Hicks and Raikhel, 2010). However, few chemical screens have been performed to facilitate a better understanding of the crosstalk between the endomembrane system and other pathways. Examples of chemicals that highlight endomembrane-trafficking crosstalk include gravacin, a compound that affect gravitropism and vacuole morphology, underscoring the link between trafficking and gravitropism (Rojas-Pierce et al., 2007), and Endosidin1, a chemical that disrupts plasma membrane transport at the tips of germinating pollen tubes and dissects endosome-mediated recycling pathways in root cells (Robert et al., 2008). A different approach based on the evolutionary conservation between plants and the yeast *Saccharomyces cerevisiae* has also been used to screen for chemicals that affect endomembrane trafficking and demonstrated that yeast can be used as a tool to identify compounds that are bioactive in plants and fungi (Zouhar et al., 2004; Chanda et al., 2009).

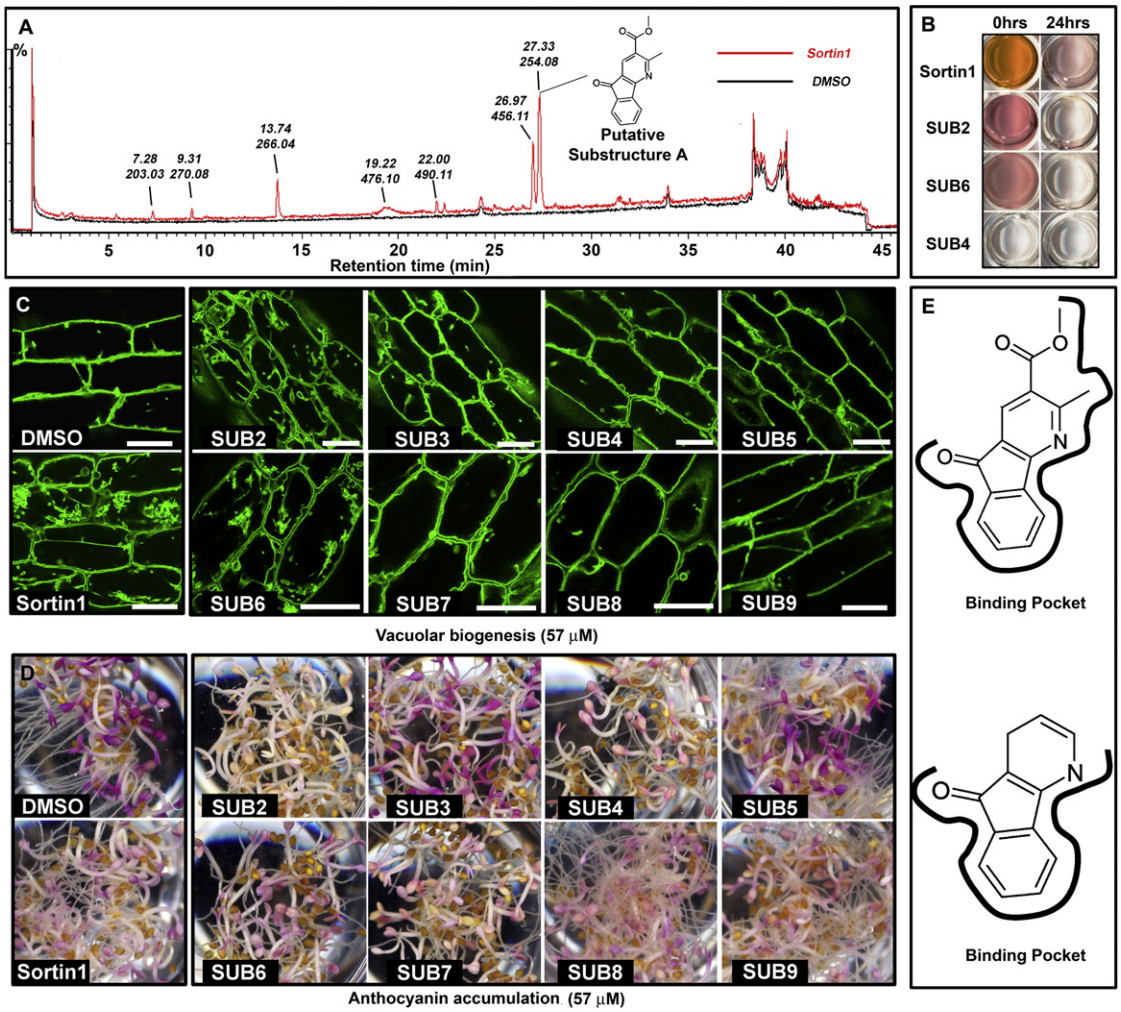

Figure 5. SAR Analyses Identify Structures Required for Sortin1 Bioactivity

(A) UPLC analysis indicates that Sortin1 is hydrolyzed in vitro (21 hr) generating lower molecular mass compounds.

(B) Color switch suggests that Sortin1-related analogs 2 and 6 (but not 4) also decompose in aqueous solutions.

(C) Effect of the Sortin1 analogs and substructures in vacuolar biogenesis. The localization of the GFP: δ-TIP marker was analyzed in seedlings grown in the absence or presence of 57 μM Sortin1, or the substructures described in Table1.

(D) Effect of the Sortin1 analogs and substructures in vacuolar-anthocyanin accumulations on AIC-grown seedlings in the absence or presence of 57 μM Sortin1, or the substructures described in Table1.

(E) Minimal bioactive substructures responsible for the vacuolar biogenesis (top) or vacuolar-anthocyanin accumulation defects (bottom).

See also Figure S4.

In this study we analyzed more in depth the phenotypic consequences of Sortin1 application in *Arabidopsis* and identified and characterized *s1h* mutants. This approach uncovered a crosstalk between the flavonoid pathway and the delivery of vacuolar cargoes mediated by vacuolar-sorting determinants in *Arabidopsis* vegetative tissues. Further support for this crosstalk was obtained by the identification of a *CHI* / *tt5* mutant allele using an independent genetic screen based on the secretion of theCLV3: T7: $CTPP_{BL}$ marker.

One of the obvious advantages of chemical genomics is that the bioactive chemicals can be directly used as reagents to probe biological pathways in a temporal and dosage-controlled manner. By using these advantages this study demonstrated that Sortin1 is a powerful inhibitor of the vacuolar accumulation of pigmented anthocyanins. In fact the chemical potency of the most bioactive Sortin1 substructures for anthocyanin-accumulation inhibition (see IC_{50} in Table 1) falls within a concentration range in which known bioactive organic molecules such as the actin-depolymerizing compound latrunculin B, the microtubule formation inhibitor oryzalin, and cellular-trafficking inhibitors, e.g., Brefeldin A and Endosidin1, are used for the dissection of endomembrane-trafficking pathways in *Arabidopsis* (Robatzek et al., 2006; Kaschani and van der Hoorn, 2007; Robert et al., 2008). However, Sortin1 differentiates from the aforementioned compounds and requires longer time to cause cellular phenotypes. This fact, together with our microarray data, suggests that *Arabidopsis* is able to generate a primary response against Sortin1-mediated stress and activate detoxification

Table 1. Bioactivity of Key Sortin1 Substructures

Chemical	Structure	Altered Vacuolar Morphology[a]	Anthocyanin-Accumulation Inhibition (IC_{50})[a]
Sortin1 (1), MW 441.4	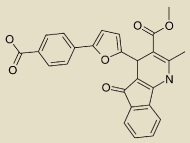	57 μM, 25 μg/ml	42 μM, 20 μg/ml
6980879 (2), MW 335.4	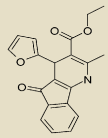	60 μM, 20 μg/ml	30 μM, 10 μg/ml
5649259 (3), MW 216.2	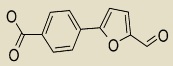	116 μM, 25 μg/ml	NA[b]
5511275 (4), MW 181.2	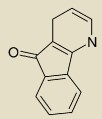	220 μM, 40 μg/ml	55 μM, 10 μg/ml
Furan (5), MW 68.1		294 μM, 40 μg/ml	NA[b]
6177037 (6), MW 441.4	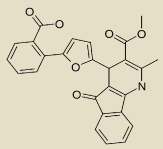	23 μM, 10 μg/ml	57 μM, 25 μg/ml
6176304 (7), MW 431.9	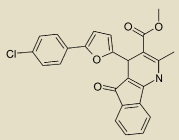	NA[b]	58 μM,[c] 25 μg/ml
6195739 (8), MW 410.3	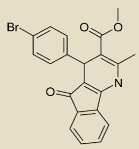	NA[b]	61 μM,[c] 25 μg/ml
6221443 (9), MW 349.4	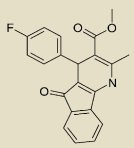	NA[b]	58 μM, 20 μg/ml

[a] Chemical potencies were defined as the minimum concentration resulting in defects in vacuole morphology, or 50% reductions in vacuolar accumulation of pigmented anthocyanin (IC_{50}).
[b] NA indicates that there was no activity in their solubility range.
[c] Compound precipitates at the concentrations indicated.

mechanisms. Apart from their direct use to dissect biological processes, the identification of cognate targets and their metabolic pathways is also informative and can be achieved by screens for resistant or hypersensitive mutants. In this study a dual hypersensitive screen for mutants with inhibited root elongation and enhanced vacuolar-biogenesis defects was used. Using this forward genetic approach, several Sortin1-hypersensitive and flavonoid-defective mutants (including the flavonoid-biosynthetic mutant *CHS* / *tt4*) were isolated. Thus, the combination of forward genetic approaches, the direct effect of Sortin1 in the vacuolar accumulation of pigmented anthocyanins, and the nearly identical flavonoid profiles of Sortin1-treated and untreated *Arabidopsis* seedlings strongly suggest that Sortin1 directly targets elements of the vacuolar-flavonoid transport pathway. In this scenario the hypersensitivity of flavonoid-defective mutants indicates that the vacuolar-flavonoid transport in Sortin1-treated plants is not totally blocked, and some flavonoid precursors are still accumulating in the vacuole.

Proposed Mechanism of Action for Sortin1

To date, only three flavonoid-defective mutants have been reported to have a role in vacuolar biogenesis in *Arabidopsis* seeds: the plasma membrane H^+-ATPase mutant *aha10*, the vacuolar flavonoid-H^+ antiporter *tt12*, and the leucoanthocyanidin dioxygenase mutant *tds4*. The phenotypes of these mutants are similar and show a predominance of multiple small vacuoles instead of a large central vacuole in the seed coat of endothelial cells (Abrahams et al., 2003; Baxter et al., 2005; Marinova et al., 2007). Based on these precedents, the identification of mutants with impaired flavonoid accumulation in a hypersensitive screen for vacuolar-biogenesis defects was not entirely surprising. However, two important conclusions derived from our chemical and genetic analyses were not previously reported. First, the mislocalization of the tonoplast δ-TIP: GFP and γ- TIP: GFP markers in the presence of Sortin1 appears to be specific, suggesting that the vacuole was the most affected organelle by the flavonoid-accumulation defects. Second, mutations in biosynthetic genes for the first two committed steps in the flavonoid pathway, the chalcone synthase (*tt4*) and the chalcone isomerase (*tt5*) mutants, were able to accumulate vacuolar cargo precursors and secrete vacuolar markers, not only in seeds but also in vegetative tissues.

To explain how defects in flavonoid transport cause aberrant distribution of vacuolar cargoes, we will focus on the last step of the process, i.e., their vacuolar uptake. At this point, it is not well understood how plants choose between ATP hydrolysis-dependent ABC transporters or H^+/ Na^+-gradient dependent for the vacuolar uptake of native metabolites (such as flavonoids) or xenobiotics (such as Sortin1). However, it is widely accepted that the conjugation of ligands, glucose, or glutathione appears to determine the transport mechanisms (Zhao and Dixon, 2010). Indeed, the same xenobiotic, if conjugated with glucose, can be taken up by a proton gradient-dependent antiporter, whereas its glutathione conjugate is taken up by an ATP-energized ABC transporter (Bartholomew et al., 2002). In our model (Figure 6), Sortin1 breaks down in aqueous solution, and the hydrophobic Substructure A crosses the plasma membrane either by diffusion or by facilitated transport. Once in the cytoplasm, Sortin1 causes oxidative stress, and Cytochrome P450-dependent monooxygenases and mixed function oxidases try to modify and inactivate the toxic compound (Rea et al., 1998) (Table S6). In the next step, the modified Substructure A is conjugated with GSH to convert it to more water-soluble forms and

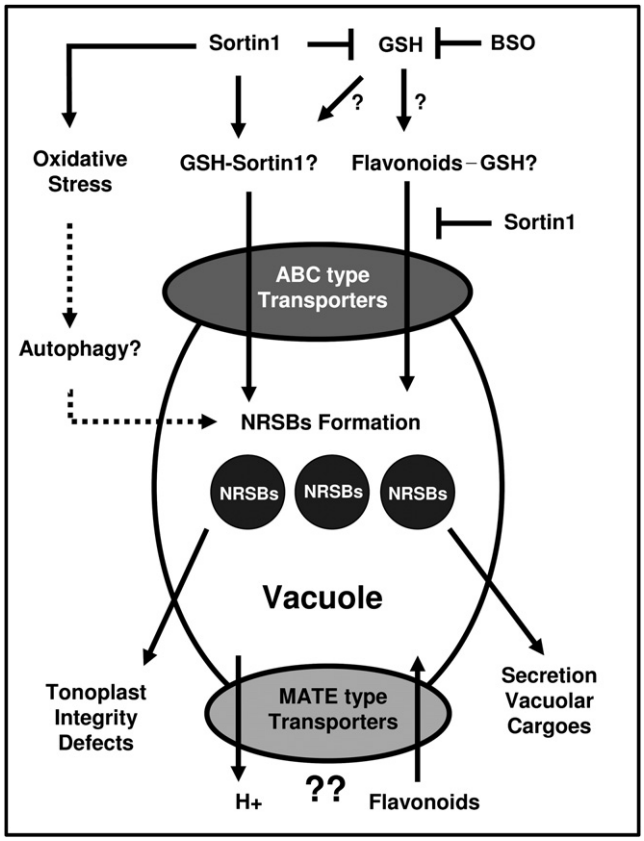

Figure 6. Model
Sortin1 generates oxidative stress, depletes the GSH pools, and inhibits the vacuolar transport of flavonoids through ABC transporters. As a consequence, tonoplast vesiculation, formation of NRSBs, and mislocalization of vacuolar-targeted cargoes are observed. Other processes such as autophagy or transport elements, e.g., MATE transporters, might also be involved.

facilitate its vacuolar sequestration (Coleman et al., 1997). In this step, Substructure A either depletes the available pool of GSH or inactivates GST enzymes, inhibiting the formation of GSH-flavonoid conjugates or GST-flavonoid complexes required for their vacuolar uptake (Marrs et al., 1995; Alfenito et al., 1998). Finally, the Substructure A-GSH conjugate is internalized and compartmentalized within the vacuole through tonoplast-localized ABC transporters (Coleman et al., 1997). In this model the combination of oxidative stress and deficient vacuolar accumulation of flavonoids might induce autophagic processes, tonoplast vesiculation, and the formation of NRSBs (Irani and Grotewold, 2005, Poustka et al., 2007, Pourcel et al., 2010). The loss of vacuolar integrity under oxidative stress conditions might in turn explain the δ-TIP: GFP mislocalization and the secretion of vacuolar-targeted cargoes. Finally, we cannot rule out an alternative model in which the phenotypes observed in Sortin1-treated seedlings are not directly due to the inhibition of the vacuolar transport of flavonoids, but the transport of cofactors or copigments required for the formation of pigmented anthocyanins in the vacuole. Thus, the current focus of our research is to determine whether GSH and other metabolites are cotransported with flavonoids, as well as to identify the putative GSH flavonoids and GSH-Sortin1 conjugates.

SIGNIFICANCE

In this report, we assign two important functions to flavonoids: as metabolites required for the maintenance of the vacuolar integrity under oxidative stress conditions, and as regulators of the delivery of vacuolar-targeted cargoes. These characteristics might be used to enhance or inhibit the accumulation of products of interest in the large central vacuole, either by genetic or chemical manipulation of the flavonoid-biosynthetic pathway. Further analysis of the Sortin1 chemical structure may provide useful information regarding the Sortin1-binding partners and may also allow the uncoupling of vacuolar cargo and flavonoid-transport pathways. More broadly, our study demonstrates that the combination of forward and reverse genetics with chemical genomics is a powerful tool to identify and dissect crosstalk between metabolic pathways.

EXPERIMENTAL PROCEDURES

Reagents and Chemical Treatments

Sortin1, analogs, and substructures were obtained from ChemBridge (San Diego, CA, USA). Analog and substructure searches utilized the Hit2Lead (ChemBridge), the SciFinder, and the ChemMine databases (http://bioweb.ucr.edu/ChemMine) (Girke et al., 2005). All chemicals were stored at −20°C as 10 mg/ml stocks in 100% DMSO. For long-term chemical treatments, seeds were surface sterilized and sown on 0.5× Murashige and Skoog media containing 0.6% Phytagar (Invitrogen) supplemented with the correspondent amounts of chemicals. After sowing, seeds were stratified at 4°C in the dark for 48 hr, then grown at 23°C with an 18-hr day cycle for 6 days. For short-term treatments, 5-day-old seedlings grown on AICs were incubated for 24 hr in liquid 0.5× Murashige and Skoog supplemented with chemicals and incubated in an orbital shaker at 100 rpm under continuous light.

Imaging

Seedling images were either produced by scanning plates on a flatbed document scanner or using a Leica MZ FLIII Stereomicroscope. To visualize fluorescent markers, confocal images of water-mounted seedlings were collected using a Leica TCS SP2/UV fitted with ×20 or ×63 water-immersion objectives. A 543 nm line from a He-Ne laser was used to excite anthocyanins, and fluorescence was detected in the 565–620 nm range. A 488 nm line from an argon laser was used to excite GFP, and fluorescence was detected in the 500–530 nm range.

Chalcone Isomerase Enzymatic Assay in *E. coli*

BL21-AI *E. coli* cells (Invitrogen) were transformed with the $TT5^{G43D}$-GST and the TT5-GST constructs. Cells were grown to an OD_{600} of 0.8–1.0 and induced with 1 mM IPTG for 3 hr. Cells were spun down, resuspended in 1× PBS, 5 mM DTT, and sonicated. The solution was cleared by centrifugation and used as the crude lysate. In vitro enzyme kinetics was carried out on 10 μl of an appropriately diluted *E. coli* crude enzyme extract per assay. Assays were done in 50 mM HEPES (pH 7.5) at 25°C using a Cary 50 Bio UV-Vis Spectrophotometer (Agilent Technologies, United States, Santa Clara, CA, USA) using the scanning kinetics function. The buffer with the extract was baselined before addition of 20–35 μM of chalcone (OD377 should be ≤1.0) into the reaction mixture. The substrate concentration in the reaction mixture was monitored at the isosbestic point at 333 nm. Velocity (dA377/min) was measured from the linear part of the graph until the substrate concentration reached isosbestic point at 333 nm and expressed as micromoles of chalcone consumed/min. Measurements were made in triplicate.

Quantification of Pigmented Anthocyanins

For experiments involving AICs in seedlings, we used the protocol established by Poustka et al. (2007) with minor modifications. For long-term chemical treatments, seedlings were directly germinated in water containing 3%

sucrose and supplemented with the different chemicals. For short-term chemical treatments, seedlings were allowed to grow for 5 days in the absence of chemicals, followed by incubations 12–24 hr in the presence of the different chemical combinations. For the quantification of pigmented anthocyanins, the preweighed *Arabidopsis* seedlings were placed into 1 ml extraction buffer (18% 1-propanol, 1% HCl, and 81% water), boiled for 3 min, and then incubated in darkness at room temperature for 8 hr in a rotary shaker. Absorbance (A_{530} and A_{657}) of the extracts was measured in a Beckman DU® 530 Spectrophotometer. The amount of anthocyanins was reported as: ($A_{530} - 0.25A_{657}$) / mg fresh weight (FW). Measurements were made in triplicate.

LC-MS Profiling of Flavonols and Anthocyanins

Frozen-ground *Arabidopsis* seedlings were extracted in 0.1% formic acid in 92% MeOH: 8% H_2O (v/v) (400 ml/100 mg tissue). The suspension was sonicated for 10 min, centrifuged at 14,000 × g for 5 min, and the obtained supernatant was filtered through a 0.22 μm PTFE membrane filter before injection to the UPLC-QTOF instrument. Analysis of metabolites was performed using the UPLC-QTOF instrument (Waters HDMS Synapt), with the UPLC column connected online to a PDA detector and then to the MS detector. The UPLC column and the chromatographic conditions were as previously described (Mintz-Oron et al., 2008). Masses of the eluted compounds (m/z range from 50 to 1500 Da) were detected with a QTOF-MS instrument equipped with an ESI source, performed in positive mode. The following settings were applied during the LC-MS runs: capillary voltage at 3 eV, cone voltage at 28 eV, and collision energy at 4 eV. For the LC-MS/MS runs, collision energies were set to 10–25 eV. A mixture of 15 standard compounds injected after each ten samples was used for quality control. The MassLynx software version 4.1 (Waters Inc.) was used to control the instrument and calculate accurate masses. QuanLynx program version 4.1 (Waters Inc.) was used for the calculation of peak areas. Metabolites were putatively identified, as described by Mintz-Oron et al. (2008).

SUPPLEMENTAL INFORMATION

Supplemental Information includes Supplemental Experimental Procedures, four figures, and six tables and can be found with this article online at doi:10.1016/j.chembiol.2010.11.015.

ACKNOWLEDGMENTS

We would like to thank Dr. G. Di Sansebastiano (Universita di Lecce), Dr. M. Grebe (Umea University), and Dr. G. Drakakaki (University of California, Davis) for their donation of the GFP: KDEL, GFP: NAG1, and CFP: SYP61 marker lines, respectively, Dr. E. Grotewold (Ohio State University) for helpful discussions, and Dr. W. van de Ven and L. Johnson for technical assistance. The Sortin1 work was supported by the NSF (MCB-0515963 to N.V.R.) and the *mtv6* mutant work by the DOE/BES Physical Biosciences program (DE–FG02–02ER15295 to N.V.R.) and by a Postdoctoral Fulbright Fellowship Award (FU– 2006–0248 to A.R.).

Received: May 29, 2010
Revised: November 23, 2010
Accepted: November 29, 2010
Published: February 24, 2011

REFERENCES

Abrahams, S., Lee, E., Walker, A., Tanner, G., Larkin, P., and Ashton, A. (2003). The *Arabidopsis* TDS4 gene encodes leucoanthocyanidin dioxygenase (LDOX) and is essential for proanthocyanidin synthesis and vacuole development. Plant J. *35*, 624–636.

Alfenito, M., Souer, E., Goodman, C., Buell, R., Mol, J., Koes, R., and Walbot, V. (1998). Functional complementation of anthocyanin sequestration in the vacuole by widely divergent glutathione S-transferases. Plant Cell *10*, 1135–1149.

Bartholomew, D., Van Dyk, D., Lau, S., O'Keefe, D., Rea, P., and Viitanen, P. (2002). Alternate energy-dependent pathways for the vacuolar uptake of glucose and glutathione conjugates. Plant Physiol. *130*, 1562–1572.

Baxter, I., Young, J., Armstrong, G., Foster, N., Bogenschutz, N., Cordova, T., Peer, W., Hazen, S., Murphy, A., and Harper, J. (2005). A plasma membrane H+-ATPase is required for the formation of proanthocyanidins in the seed coat endothelium of *Arabidopsis thaliana*. Proc. Natl. Acad. Sci. USA *102*, 2649–2654.

Chanda, A., Roze, L., Kang, S., Artymovich, K., Hicks, G., Raikhel, N., Calvo, A., and Linz, J. (2009). A key role for vesicles in fungal secondary metabolism. Proc. Natl. Acad. Sci. USA *106*, 19533–19538.

Coleman, J.O.D., Randall, R., and Blake-Kalff, M.M.A. (1997). Detoxification of xenobiotics in plant cells by glutathione conjugation and vacuolar compartmentalization: a fluorescent assay using monochlorobimane. Plant Cell Environ. *20*, 449–460.

Cutler, S., Ehrhardt, D., Griffitts, J., and Somerville, C. (2000). Random GFP:cDNA fusions enable visualization of subcellular structures in cells of *Arabidopsis* at a high frequency. Proc. Natl. Acad. Sci. USA *97*, 3718–3723.

Dana, C.D., Bevan, D.R., and Winkel, B.S. (2006). Molecular modeling of the effects of mutant alleles on chalcone synthase protein structure. J. Mol. Model. *12*, 905–914.

Fluckiger, R., De Caroli, M., Piro, G., Dalessandro, G., Neuhaus, J., and Di Sansebastiano, G. (2003). Vacuolar system distribution in *Arabidopsis* tissues, visualized using GFP fusion proteins. J. Exp. Bot. *54*, 1577–1584.

Gandia-Herrero, F., Lorenz, A., Larson, T., Graham, I., Bowles, D., Rylott, E., and Bruce, N. (2008). Detoxification of the explosive 2,4,6-trinitrotoluene in *Arabidopsis*: discovery of bifunctional O- and C-glucosyltransferases. Plant J. *56*, 963–974.

Girke, T., Cheng, L., and Raikhel, N. (2005). ChemMine. A compound mining database for chemical genomics. Plant Physiol. *138*, 573–577.

Grebe, M., Xu, J., Möbius, W., Ueda, T., Nakano, A., Geuze, H.J.., Rook, M.B., and Scheres, B. (2003). *Arabidopsis* sterol endocytosis involves actin-mediated trafficking via ARA6-positive early endosomes. Curr. Biol. *13*, 1378–1387.

Hicks, G.R., and Raikhel, N.V. (2010). Advances in dissecting endomembrane trafficking with small molecules. Curr. Opin. Plant Biol. *13*, 706–713.

Hicks, G.R., Rojo, E., Hong, S., Carter, D.G., and Raikhel, N.V. (2004). Geminating pollen has tubular vacuoles, displays highly dynamic vacuole biogenesis, and requires VACUOLESS1 for proper function. Plant Physiol. *134*, 1227–1239.

Horazdovsky, B., and Emr, S. (1993). The VPS16 gene product associates with a sedimentable protein complex and is essential for vacuolar protein sorting in yeast. J. Biol. Chem. *268*, 4953–4962.

Irani, N.G., and Grotewold, E. (2005). Light-induced morphological alteration in anthocyanin-accumulating vacuoles of maize cells. BMC Plant Biol. *5*, 7.

Jez, J., Bowman, M., Dixon, R., and Noel, J. (2000). Structure and mechanism of the evolutionarily unique plant enzyme chalcone isomerase. Nat. Struct. Biol. *7*, 786–791.

Kaschani, F., and van der Hoorn, R. (2007). Small molecule approaches in plants. Curr. Opin. Chem. Biol. *11*, 88–98.

Koprivova, A., Mugford, S., and Kopriva, S. (2010). *Arabidopsis* root growth dependence on glutathione is linked to auxin transport. Plant Cell Rep. *29*, 1157–1167.

Lepiniec, L., Debeaujon, I., Routaboul, J., Baudry, A., Pourcel, L., Nesi, N., and Caboche, M. (2006). Genetics and biochemistry of seed flavonoids. Annu. Rev. Plant Biol. *57*, 405–430.

Marinova, K., Pourcel, L., Weder, B., Schwarz, M., Barron, D., Routaboul, J., Debeaujon, I., and Klein, M. (2007). The *Arabidopsis* MATE transporter TT12 acts as a vacuolar flavonoid/H+ -antiporter active in proanthocyanidin-accumulating cells of the seed coat. Plant Cell *19*, 2023–2038.

Marrs, K., Alfenito, M., Lloyd, A., and Walbot, V. (1995). A glutathione S-transferase involved in vacuolar transfer encoded by the maize gene Bronze-2. Nature *375*, 397–400.

Martens, S., Preuss, A., and Matern, U. (2010). Multifunctional flavonoid dioxygenases: flavonol and anthocyanin biosynthesis in *Arabidopsis thaliana L.* Phytochemistry *71*, 1040–1049.

Mintz-Oron, S., Mandel, T., Rogachev, I., Feldberg, L., Lotan, O., Yativ, M., Wang, Z., Jetter, R., Venger, I., Adato, A., et al. (2008). Gene expression and metabolism in tomato fruit surface tissues. Plant Physiol. *147*, 823–851.

Norambuena, L., Zouhar, J., Hicks, G.R., and Raikhel, N.V. (2008). Identification of cellular pathways affected by Sortin2, a synthetic compound that affects protein targeting to the vacuole in Saccharomyces cerevisiae. BMC Chem. Biol. *8*, 1.

Park, S., Fung, P., Nishimura, N., Jensen, D., Fujii, H., Zhao, Y., Lumba, S., Santiago, J., Rodrigues, A., Chow, T., et al. (2009). Abscisic acid inhibits type 2C protein phosphatases via the PYR/PYL family of START proteins. Science *324*, 1068–1071.

Peer, W., and Murphy, A. (2007). Flavonoids and auxin transport: modulators or regulators? Trends Plant Sci. *12*, 556–563.

Pourcel, L., Routaboul, J., Cheynier, V., Lepiniec, L., and Debeaujon, I. (2007). Flavonoid oxidation in plants: from biochemical properties to physiological functions. Trends Plant Sci. *12*, 29–36.

Pourcel, L., Irani, N.G., Lu, Y., Riedl, K., Schwartz, S., and Grotewold, E. (2010). The formation of anthocyanic vacuolar inclusions in *Arabidopsis thaliana* and implications for the sequestration of anthocyanin pigments. Mol. Plant *3*, 78–90.

Poustka, F., Irani, N., Feller, A., Lu, Y., Pourcel, L., Frame, K., and Grotewold, E. (2007). A trafficking pathway for anthocyanins overlaps with the endoplasmic reticulum-to-vacuole protein-sorting route in *Arabidopsis* and contributes to the formation of vacuolar inclusions. Plant Physiol. *145*, 1323–1335.

Rabino, I., and Mancinelli, A.L. (1986). Light, temperature, and anthocyanin production. Plant Physiol. *81*, 922–924.

Rea, P., Li, Z., Lu, Y., Drozdowicz, Y., and Martinoia, E. (1998). From vacuolar GS-X pumps to multispecific ABC transporters. Annu. Rev. Plant Physiol. Plant Mol. Biol. *49*, 727–760.

Robatzek, S., Chinchilla, D., and Boller, T. (2006). Ligand-induced endocytosis of the pattern recognition receptor FLS2 in *Arabidopsis*. Genes Dev. *20*, 537–542.

Robert, S., Chary, S., Drakakaki, G., Li, S., Yang, Z., Raikhel, N., and Hicks, G. (2008). Endosidin1 defines a compartment involved in endocytosis of the brassinosteroid receptor BRI1 and the auxin transporters PIN2 and AUX1. Proc. Natl. Acad. Sci. USA *105*, 8464–8469.

Rojas-Pierce, M., Titapiwatanakun, B., Sohn, E., Fang, F., Larive, C., Blakeslee, J., Cheng, Y., Cutler, S., Cuttler, S., Peer, W., et al. (2007). *Arabidopsis* P-glycoprotein19 participates in the inhibition of gravitropism by gravacin. Chem. Biol. *14*, 1366–1376.

Rojo, E., Gillmor, C., Kovaleva, V., Somerville, C., and Raikhel, N. (2001). VACUOLELESS1 is an essential gene required for vacuole formation and morphogenesis in *Arabidopsis*. Dev. Cell *1*, 303–310.

Rosado, A., Sohn, E., Drakakaki, G., Pan, S., Swidergal, A., Xiong, Y., Kang, B., Bressan, R., and Raikhel, N. (2010). Auxin-mediated ribosomal biogenesis regulates vacuolar trafficking in *Arabidopsis*. Plant Cell *22*, 143–158.

Sanderfoot, A., Pilgrim, M., Adam, L., and Raikhel, N. (2001). Disruption of individual members of *Arabidopsis* syntaxin gene families indicates each has essential functions. Plant Cell *13*, 659–666.

Shirley, B., Kubasek, W., Storz, G., Bruggemann, E., Koornneef, M., Ausubel, F., and Goodman, H. (1995). Analysis of *Arabidopsis* mutants deficient in flavonoid biosynthesis. Plant J. *8*, 659–671.

Steinkellner, S., Lendzemo, V., Langer, I., Schweiger, P., Khaosaad, T., Toussaint, J.P., and Vierheilig, H. (2007). Flavonoids and strigolactones in root exudates as signals insymbiotic and pathogenic plant-fungus interactions. Molecules *5*, 1290–1306.

Sohn, E., Rojas-Pierce, M., Pan, S., Carter, C., Serrano-Mislata, A., Madueño, F., Rojo, E., Surpin, M., and Raikhel, N. (2007). The shoot meristem identity gene TFL1 is involved in flower development and trafficking to the protein storage vacuole. Proc. Natl. Acad. Sci. USA *104*, 18801–18806.

Surpin, M., and Raikhel, N. (2004). Traffic jams affect plant development and signal transduction. Nat. Rev. Mol. Cell Biol. *5*, 100–109.

Surpin, M., Zheng, H., Morita, M., Saito, C., Avila, E., Blakeslee, J., Bandyopadhyay, A., Kovaleva, V., Carter, D., Murphy, A., et al. (2003). The VTI family of SNARE proteins is necessary for plant viability and mediates different protein transport pathways. Plant Cell *15*, 2885–2899.

Taylor, L., and Grotewold, E. (2005). Flavonoids as developmental regulators. Curr. Opin. Plant Biol. *8*, 317–323.

Treutter, D. (2005). Significance of flavonoids in plant resistance and enhancement of their biosynthesis. Plant Biol. (Stuttg.) *7*, 581–591.

Winkel, B. (2004). Metabolic channeling in plants. Annu. Rev. Plant Biol. *55*, 85–107.

Winkel-Shirley, B. (2001). Flavonoid biosynthesis. A colorful model for genetics, biochemistry, cell biology, and biotechnology. Plant Physiol. *126*, 485–493.

Yazaki, K. (2006). ABC transporters involved in the transport of plant secondary metabolites. FEBS Lett. *580*, 1183–1191.

Zhao, J., and Dixon, R. (2010). The 'ins' and 'outs' of flavonoid transport. Trends Plant Sci. *15*, 72–80.

Zhao, J., Pang, Y., and Dixon, R. (2010). The mysteries of proanthocyanidin transport and polymerization. Plant Physiol. *153*, 437–443.

Zouhar, J., Hicks, G., and Raikhel, N. (2004). Sorting inhibitors (Sortins): chemical compounds to study vacuolar sorting in *Arabidopsis*. Proc. Natl. Acad. Sci. USA *101*, 9497–9501.